Journal of Alloys and Compounds 506 (2010) 516–519

Contents lists available at ScienceDirect

Journal of Alloys and Compounds

journal homepage: www.elsevier.com/locate/jallcom

Martensitic transition and magnetocaloric properties in $Ni_{45}Mn_{44-x}Fe_xSn_{11}$ alloys

J.L. Yan[a,b,*], Z.Z. Li[a,b], X. Chen[a,b], K.W. Zhou[a,b], S.X. Shen[a,b], H.B. Zhou[a,b]

[a] College of Materials Science and Engineering, Guangxi University, Nanning, Guangxi 530004, PR China
[b] Key Laboratory of Nonferrous Metal Materials and New Processing Technology, Ministry of Education, Guangxi University, Nanning, Guangxi 530004, PR China

ARTICLE INFO

Article history:
Received 30 April 2010
Received in revised form 7 July 2010
Accepted 9 July 2010
Available online 15 July 2010

Keywords:
Transition metal alloys and compounds
Martensitic transition
Magnetocaloric effect
Magnetic measurements

ABSTRACT

The structural, martensitic transition and magnetocaloric effect in Heusler alloys $Ni_{45}Mn_{44-x}Fe_xSn_{11}$ (x = 0, 2, 5 and 8) have been studied by means of XRD, SEM/EDS and magnetization measurements. The alloys with x = 2 and 5 exhibit the co-existence of orthorhombic (S.G. *Pmma*) martensite phase and cubic $L2_1$ structure (S.G. *Fm-3m*) austenite phase at room temperature. The martensitic transition temperature, M_s, shows a non-monotonic dependence on the Fe content. M_s increases from 265 K in the undoped alloy to 310 K with the addition of 2 at.% Fe, whereas further increase in Fe content to 5 and 8 at.% leads to the decrease of M_s to 290 and 207 K. Substitution of Fe for Mn slightly increases the Curie temperature of austenite phase and the thermal hysteresis. Associated with the martensitic transition, the maximum magnetic entropy changes under a magnetic field change of 20 kOe are 10.6, 6.4 and 5.6 J/kg K for x = 0, 5 and 8, respectively.

1. Introduction

Magnetic refrigeration based on the magnetocaloric effect (MCE) is expected to be an alternative to the conventional gas compression refrigeration for room temperature applications in view of energy saving and environmental friendliness. The MCE is usually measured in terms of isothermal magnetic entropy change (ΔS_M) or adiabatic temperature change (ΔT_{ad}). Since the discovery of giant MCE in $Gd_5Si_2Ge_2$ [1,2], the search for magnetic materials with large ΔS_M near room temperature as potential magnetic refrigerants has been intense. The magnetocaloric materials found so far can be classified into two categories, one is the rare earth-based compounds such as $Gd_5(Si_xGe_{1-x})_4$ [2] and $La(Fe_{13-x}Si_x)$ [3], the other is the Mn-based compounds such as $Mn(As_{1-x}Sb_x)$ [4], $MnFe(P_{1-x}As_x)$ [5] and Ni_2MnGa [6]. Recently the Mn-based compounds have attracted increasing attention because of the abundant resource of manganese and therefore relatively low cost as compared with the rare earth elements.

It has been demonstrated that the non-stoichiometric Ni–Mn–Sn Heusler alloy exhibits both structural and magnetic transitions [7]. Upon cooling the alloy undergoes a martensitic transition (MT) from a parent austenite phase with a cubic $L2_1$-type structure (space group *Fm-3m*) to a martensite phase, accompanying an abrupt drop in magnetization. The martensitic phase may appear as various modulated structures, evolved from the cubic parent phase to 10 M, 14 M, or $L1_0$ structure with the increase in the valence electron concentration per atom e/a [7–9]. Large positive ΔS_M is reported to be associated with the first-order MT, while relatively smaller negative ΔS_M be associated with the second-order ferromagnetic (FM) to paramagnetic (PM) transition [7,10,11]. Therefore, to be a potential candidate for magnetic refrigerants, it is favorable for the alloys to have the MT occurred near room temperature. It is reported that the MT temperature in the Ni–Mn–Sn alloys can be adjusted by varying the composition ratios of Ni:Mn:Sn [10,11] or adding doping elements such as Cr, Fe, Co, Cu for Ni [12–14] or Mn [15–20]. In the case of partial substitution of Fe for Mn, more recently two studies about the martensitic transition and magnetic entropy change in Ni–Mn–Sn alloys were found [15,21]. Passamani et al. [15] reported that the dopant of Fe results in a decrease in the MT temperature and an increase in Curie temperature of the austenitic phase in $Ni_{50}(Mn_{1-x}Fe_x)_{36}Sn_{14}$ (x = 0, 0.03, 0.07, 0.10 and 0.15) alloys, whereas Han et al. [21] reported that the dopant of Fe results in an increase in the MT temperature in $Ni_{43}Mn_{46-x}Fe_xSn_{11}$ (x = 0, 2 and 4) alloys. In this paper, we report on the effect of substitution of Fe for Mn on the martensitic transition and magnetocaloric effect in $Ni_{45}Mn_{44-x}Fe_xSn_{11}$ alloys.

2. Experimental

Ingots of 4 g each with nominal composition $Ni_{45}Mn_{44-x}Fe_xSn_{11}$ (x = 0, 2, 5 and 8) were prepared from purity (99.9.%) elements by arc melting under high purity argon atmosphere in a water-cooled copper hearth. 1 wt.% excess of Mn was added to compensate the evaporation loss during arc melting. The sample was turned over and re-melted five times to ensure a good homogeneity. The obtained ingots were sealed

* Corresponding author at: College of Materials Science and Engineering, Guangxi University, Nanning, Guangxi 530004, PR China. Tel.: +86 771 3233530; fax: +86 771 3233530.
E-mail address: yjl@gxu.edu.cn (J.L. Yan).

0925-8388/$ – see front matter © 2010 Elsevier B.V. All rights reserved.
doi:10.1016/j.jallcom.2010.07.076

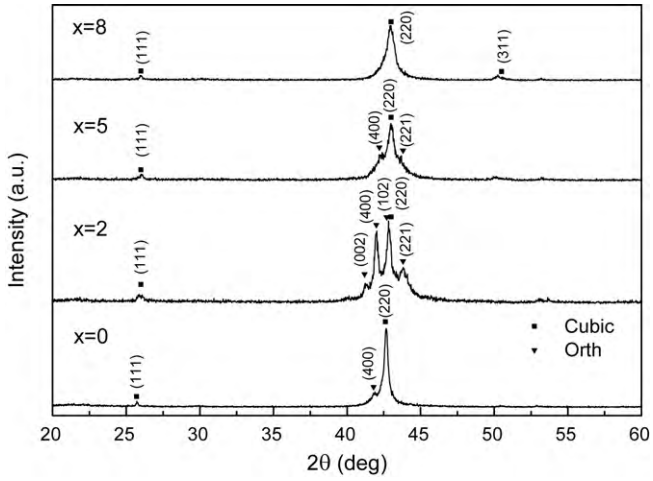

Fig. 1. X-ray diffraction patterns of $Ni_{45}Mn_{44-x}Fe_xSn_{11}$ (x = 0, 2, 5 and 8) alloys recorded at room temperature.

in a quartz tube of high vacuum, annealed at 900 °C for 10 days, and then quenched in liquid nitrogen. The compositions of the alloys were checked using a Hitachi S-3400N scanning electron microscope (SEM) equipped with an EDAX energy dispersive X-ray spectrometer (EDS). Powder X-ray diffraction (XRD) was performed on a Rigaku D/Max 2500 V diffractometer using Cu Kα radiation and graphite monochromator. Magnetic measurements were carried out using a Lakeshore 7410 vibrating sample magnetometer. The temperature dependence of the magnetization was measured in an external magnetic field of 500 Oe. A thermal protocol was followed: the sample was firstly cooled down to 80 K in a zero field, subsequently an external field was applied and the measurements were taken on increasing temperature up to 400 K, giving the zero-field-cooled state (ZFC) heating curve. Then the field-cooled (FC) curve from 400 to 80 K was measured in the same field. The isothermal magnetization curves were recorded at different temperatures with a maximum magnetic field of 20 kOe. Temperature intervals were 2 K in the vicinity of the MT and Curie temperatures, and 5 or 10 K elsewhere. The isothermal magnetic entropy change ΔS_M was calculated from isothermal magnetization curves using the Maxwell relation:

$$\Delta S_M = \int_0^H \left(\frac{\partial M(H,T)}{\partial T}\right)_H dH \quad (1)$$

For magnetization measured at discrete field and temperature intervals, ΔS_M was approximated by numerical integration of two consecutive magnetization isotherms as follows:

$$\Delta S_M = \frac{1}{\Delta T}\left[\int_0^H M(T+\Delta T,H)dH - \int_0^H M(T,H)dH\right] \quad (2)$$

3. Results and discussion

3.1. Structure

Fig. 1 shows the XRD patterns of $Ni_{45}Mn_{44-x}Fe_xSn_{11}$ alloys with x = 0, 2, 5 and 8 taken at room temperature. The alloy with x = 8 is a single austenite phase with a cubic Heusler $L2_1$ structure, space group *Fm-3m* and lattice parameter 0.5939 nm. The XRD patterns for x = 2 and 5 show the co-existence of martensite and austenite phases, with the martensite being minor phase for x = 5. The reflection peaks of the martensite phase correspond well with the calculated Bragg peaks based on the orthorhombic martensite structure (space group *Pmma*) determined by neutron powder diffraction [8]. The alloy with x = 0 is essentially austenite phase with trace second phase being identified as the orthorhombic martensite phase. By replacing Mn with Fe, which has a smaller atomic radius than Mn, the reflection peaks of the cubic phase shift to a higher angle and the lattice shrinks. The lattice parameters for the austenite phase are listed in Table 1. It is seen that the lattice parameters is almost the same for x = 5 and 8, indicating that the amount of Fe is out of its solid solubility limit in the $L2_1$ type Ni_2MnSn compound.

The SEM/EDS examinations indicated that the overall compositions of the alloys determined by EDS are close to the nominal ones. Each measured composition listed in Table 1 was taken as the average of four measurements. The standard deviations for EDS are less than ±0.6 at.% for Ni, ±0.5 at.% for Mn, ±0.3 at.% for Sn and ±0.3 at.% for Fe. The coefficients of variation between these measurements are maximum 1.4% for Ni, 1.4% for Mn, 2.8% for Sn and 7.6% for Fe. The discrepancies between the nominal and measured composition for Mn and Fe elements are thought to be associated with the partial overlap of Fe K_α peak and Mn K_β peak in the EDS spectrum. Except for the matrix phase, a Mn-rich phase was found from EDS analysis in all alloys, and a coarse (MnNiFe)-rich phase which indicates the segregation of the solute atoms was found in the alloys with x = 5 and 8. The segregation of Ni, Mn and Fe reduces the concentrations of these elements in the matrix.

3.2. Martensitic transition and magnetocaloric effect

The temperature dependence of the magnetization curves, M–T curves, which measured on the heating and cooling processes in a magnetic field of 500 Oe for $Ni_{45}Mn_{44-x}Fe_xSn_{11}$ (x = 0, 2, 5 and 8) are presented in Fig. 2. The martensitic start and finish temperatures (M_s, M_f), austenitic start and finish temperatures (A_s, A_f) are defined from the heating and cooling curves. The Curie temperatures of martensitic phase (T_C^M) and austenitic phase (T_C^A) were determined from the minima in the temperature derivative of the magnetization dM/dT versus T curves. These data are collected in Table 1. It is observed from the cooling curves in Fig. 2a, c and d that with the decreasing of the temperature, the alloy which at first is in the austenitic PM state, undergoes a magnetic transition from PM to FM state around T_C^A and obtains a large magnetization. The ferromagnetism extends to M_s temperature, then the magnetization drops sharply, corresponding to the martensitic transition and the alloy is in a weak-magnetic martensitic state (Fig. 2a and c) or in the martensitic FM state (Fig. 2d). Subsequently a PM to FM transition of the martensitic phase occurs around T_C^M as the temperature is further decreased. In these alloys the magnetization of the austenitic FM state is higher than that of the martensitic FM state. A thermal hysteresis (ΔT) of about 15 K and 20 K around the martensitic transition is observed for x = 5 and 8, demonstrating a first-order structural transition. The ΔT values of the Fe-doped alloys are slightly larger than that of the undoped alloy (10 K). It is found that the magnetization of the alloys with x = 5 and 8 in the austenitic PM state do not approach zero, which indicates the existence of a second magnetic phase. This is in good agreement with the results of SEM/EDS. For the alloy with x = 2, it is seen

Table 1
The measured composition, valence electron concentration (e/a), lattice parameter for the austenitic phase, martensitic start and finish temperatures (M_s, M_f), austenitic start and finish temperatures (A_s, A_f), Curie temperatures of martensitic (T_C^M) and austenitic phase (T_C^A), magnetic entropy change around the MT ($+\Delta S_M$) and T_C^A ($-\Delta S_M$) for the $Ni_{45}Mn_{44-x}Fe_xSn_{11}$ alloys.

x	Composition measured by EDS	e/a	Lattice parameter a (nm)	T_C^M (K)	M_s (K)	M_f (K)	A_s (K)	A_f (K)	T_C^A (K)	$+\Delta S_M$ (J/kg K)	$-\Delta S_M$ (J/kg K)
0	$Ni_{44.4}Mn_{44.1}Sn_{11.5}$	7.99	0.5992	170	265	255	265	275	285	10.6	−1.7
2	$Ni_{43.8}(Mn_{42.3}Fe_{2.6})Sn_{11.3}$	8.00	0.5970	150	310	–	310	325	–	–	–
5	$Ni_{44.2}(Mn_{39.3}Fe_{4.9})Sn_{11.6}$	8.03	0.5935	225	290	278	292	298	298	6.4	−1.0
8	$Ni_{44.5}(Mn_{37.0}Fe_{6.7})Sn_{11.8}$	8.05	0.5939	–	207	179	180	228	312	5.6	−1.2

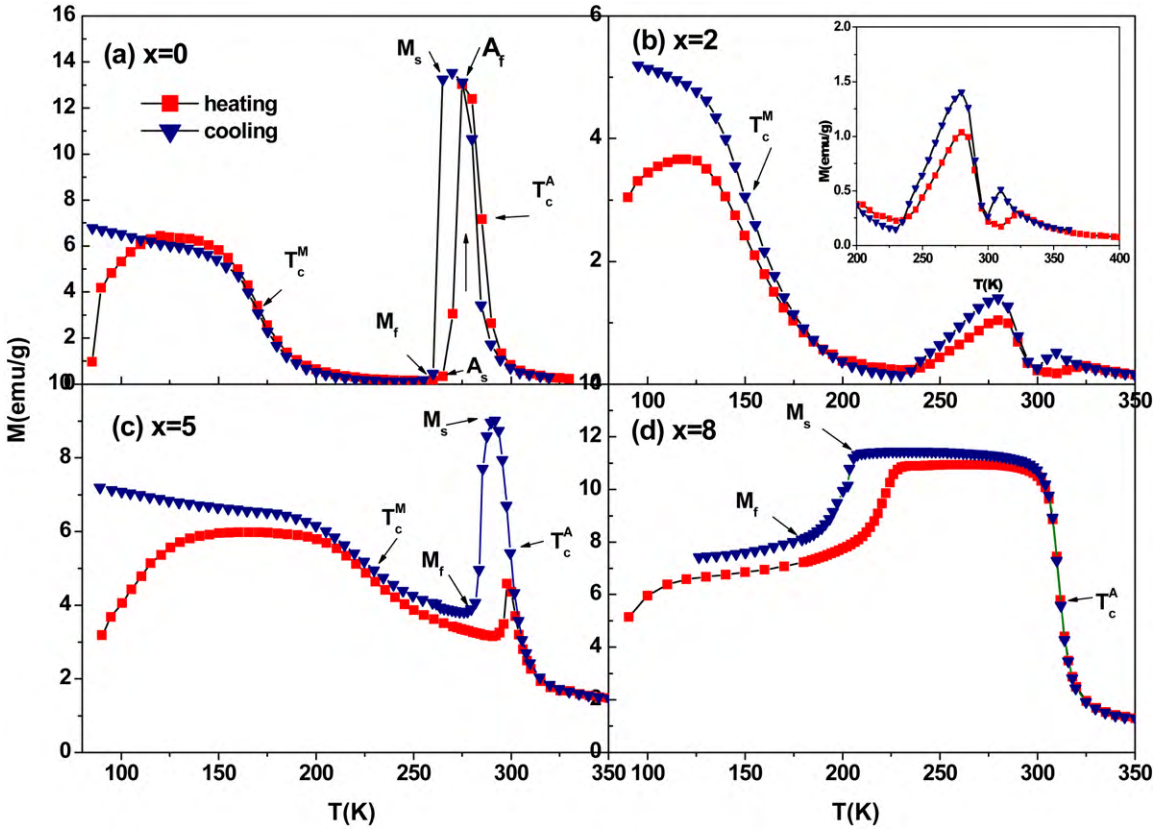

Fig. 2. Temperature dependence of magnetization for $Ni_{45}Mn_{44-x}Fe_xSn_{11}$ (x = 0, 2, 5 and 8) alloys under an applied magnetic field of 500 Oe on heating and cooling.

from Fig. 2b that the MT takes place near room temperature at M_s = 310 K where both the martensitic and austenitic phases are in the PM state. In addition, a hump which lies between 230 and 300 K is observed in Fig. 2b. Considering the obvious different magnetic characteristic of this alloy with the others (Fig. 2a, c and d), the homogeneity of the sample for x = 2 was checked by two independent powder XRD measurements on different pieces cut from the ingot. The obtained two XRD patterns for x = 2 are the same, clearly indicating the coexistence of the martensite and the austenite phases. Three independent M–T measurements for x = 2 were also carried out on different specimens of about 20 mg, with one of the specimen taken from the metallographic specimen used for EDS determination (and its M–T curve is presented in Fig. 2b). It was found that two of these three M–T measurements gave the identical results, as shown in Fig. 2b; while one M–T measurement showed the absence of the hump. To clarify this magnetic behavior, further investigation is required. It is suggested that the hump can be associated with an intermartensitic transition. Such a martensitic to martensitic transition has been observed in Ni–Mn–x (x = In, Sn, Sb) alloys [22]. Nevertheless, the results obtained from the analysis of the M–T curves are consistent with the XRD results.

As seen from Fig. 2 and Table 1, the T_C^A value increases with the increase in Fe content. The change in M_s is complex. The M_s value for the alloy with x = 0 is 265 K, which is in good agreement with that reported by Han et al. [11]. With the addition of 2 at.% Fe, M_s increases to 310 K. However, M_s shifts to lower temperature of 290 and 207 K with further increasing Fe content to 5 and 8 at.%. Similar behavior of the composition dependence of M_s has been observed in Cu-doped $Ni_{50}Mn_{35-x}Cu_xSn_{15}$ (x = 2, 5 and 10) alloys [20] and $Ni_{43}Mn_{46-x}Cu_xSn_{11}$ (x = 1, 2 and 3) alloys [16]. The MT temperature increases with the Cu content for up to 3 at.% Cu [16], and then decreases rapidly with further increasing Cu content to 10 at.% [20]. It has been shown that M_s for the Ni–Mn–Sn alloys is related to the e/a [7,14,16,18]. As a rule of thumb, the e/a theory, i.e. M_s increases with increasing value of e/a, was applied to estimate the trend of the variation in M_s. The e/a values for the alloys studied were calculated using the EDS measured alloy composition, as tabulated in Table 1. Here the number of valence electrons per atom for Ni, Mn, Sn and Fe atoms are 10 (3d8 4s2), 7 (3d5 4s2), 4 (5s2 5p2) and 8 (3d6 4s2), respectively. From Table 1, it is found that the empirical relationship between M_s and e/a could not explain the variation of M_s in our Fe-doping alloys. Combining our results with that reported by Passamani et al. [15] and Han et al. [21], it is thought that other factors than the e/a value, such as the site occupancy, the actual crystallographic structure of the martensitic phase and its grain size, and the stress field caused by substitution should be taken into account for a clear understanding of the change in M_s by doping elements.

Fig. 3 shows the isothermal magnetization curves for the alloys with x = 5 and 8 measured in a sequence of decreasing temperature under a magnetic field of 0–20 kOe. With decreasing temperature from 350 K to 293 K, the magnetization in Fig. 3a increases steadily and reaches a maximum at 291 K as the austenite orders ferromagnetically at the Curie temperature. The magnetization then decreases unevenly to 250 K as the structure transforms from austenite to martensite. It is seen that a large change in magnetization between two consecutive isotherms occurs at the martensitic transition, e.g. between 287 and 285 K for x = 5. Calculated from the magnetization isotherms using Eq. (2), the temperature dependence of ΔS_M in the magnetic field change between 0 and 20 kOe for x = 0, 5 and 8 are presented in Fig. 4. The maximum values of ΔS_M are listed in Table 1. It is found from Figs. 2 to 4 that a large MCE can be obtained in the vicinity of the MT, resulting from an abrupt drop in magnetization between M_s and M_f temperatures. Different from the strongly composition dependence of the M_s, the maximum values of ΔS_M associated with the MT are found to be weakly dependent of the Fe content and are 10.6, 6.4 and 5.6 J/kg K

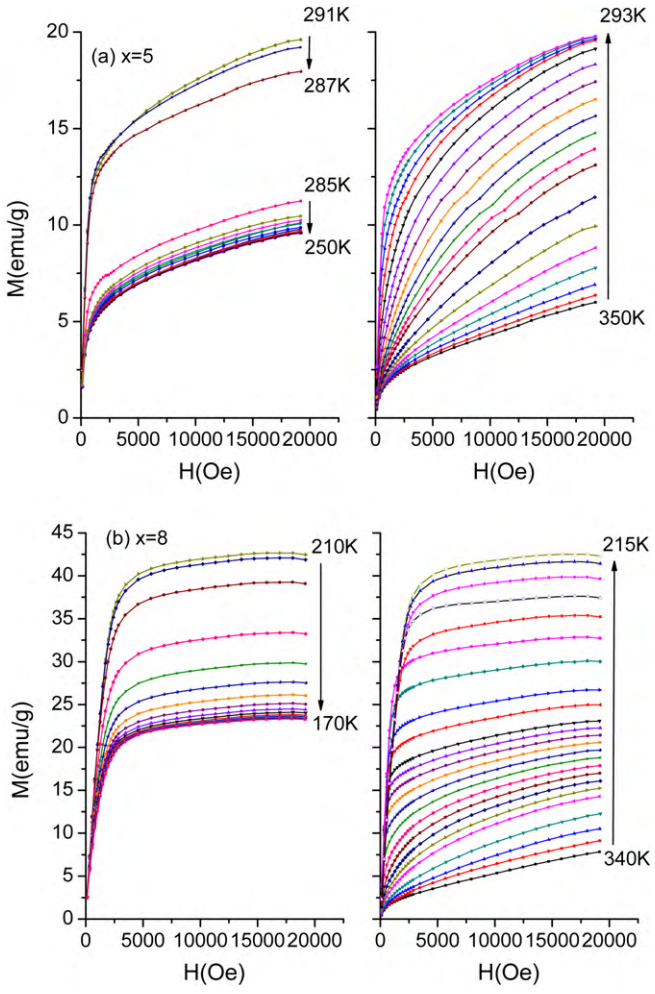

Fig. 3. Isothermal magnetization curves for $Ni_{45}Mn_{44-x}Fe_xSn_{11}$ ($x = 5, 8$) alloys measured in the magnetic field range of 0–20 kOe: (a) $x = 5$ and (b) $x = 8$.

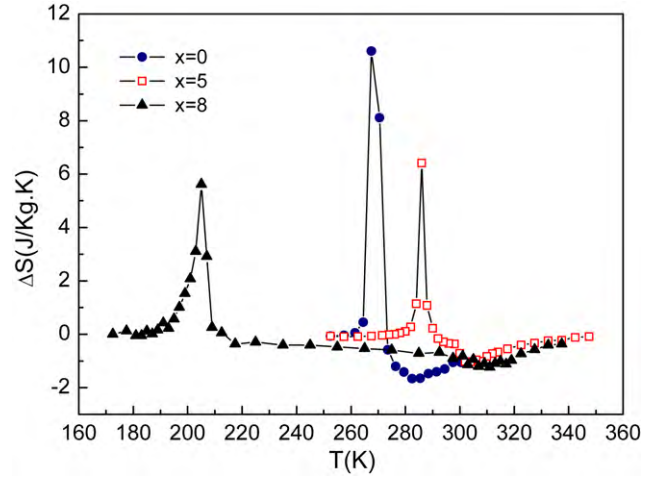

Fig. 4. Temperature dependence of magnetic entropy change ΔS_M in the magnetic field change of 0–20 kOe for $Ni_{45}Mn_{44-x}Fe_xSn_{11}$ ($x = 0, 5, 8$) alloys.

for $x = 0$, 5 and 8, respectively. These features are of technological importance, and $Ni_{45}(Mn_{44-x}Fe_x)Sn_{11}$ alloys with Fe content less than 5 at.% may be considered as promising near room temperature MCE materials. Small negative peaks are seen around the T_C^A temperatures. The magnetic properties in the Mn-based Heusler alloys are mainly attributed to the Mn magnetic moments and thus the Mn–Mn distance. It is proposed that the presence of short-range antiferromagnetic ordering between Mn atoms in the martensitic phase is responsible for the magnetization drop around the martensitic transition, and therefore for the large MCE [8,13].

4. Conclusions

The effect of the substitution of Fe for Mn on structure, martensitic transition and magnetic entropy change in the $Ni_{45}Mn_{44-x}Fe_xSn_{11}$ alloys has been investigated. XRD and SEM/EDS results revealed that the solubility limit of Fe in $L2_1$ type structure $Ni_{45}Mn_{44}Sn_{11}$ is less than 5 at.% Fe. The variation in MT temperature with the amount of Fe substitution for Mn is complex. Replacing Mn by Fe increases the Curie temperature of austenitic phase and slightly increases the thermal hysteresis by 5–10 K. The values of maximum magnetic entropy change in the vicinity of the MT are insensitive to the Fe content. The ΔS_M for alloy $Ni_{45}(Mn_{39}Fe_5)Sn_{11}$ is 6.4 J/kg K at 286 K for a magnetic field change of 20 kOe.

Acknowledgements

This work was supported by the National Natural Science Foundation of China (No. 50861004) and the Doctoral Scientific Research Foundation of Guangxi University (No. X071028).

References

[1] K.A. Gschneidner, V.K. Pecharsky, A.O. Tsokol, Rep. Prog. Phys. 68 (2005) 1479–1539.
[2] V.K. Pecharsky, K.A. Gschneidner Jr., Phys. Rev. Lett. 78 (1997) 4494–4497.
[3] B.G. Shen, J.R. Sun, F.X. Hu, H.W. Zhang, Z.H. Cheng, Adv. Mater. 21 (2009) 4545–4564.
[4] H. Wada, Y. Tanabe, Appl. Phys. Lett. 79 (2001) 3302–3304.
[5] O. Tegus, E. Bruck, K.H.J. Buschow, F.R. de Boer, Nature (London) 415 (2002) 150–152.
[6] F.-X. Hu, B.-G. Shen, J.-R. Sun, Appl. Phys. Lett. 76 (2000) 3460.
[7] T. Krenke, M. Acet, E.F. Wassermann, X. Moya, L. Manosa, A. Planes, Phys. Rev. B 72 (2005) 014412.
[8] P.J. Brown, A.P. Gandy, K. Ishida, R. Kainuma, T. Kanomata, K.U. Neumann, K. Oikawa, B. Ouladdiaf, K.R.A. Ziebeck, J. Phys.: Condens. Matter 18 (2006) 2249–2259.
[9] A. Planes, L. Manosa, M. Acet, J. Phys.: Condens. Matter 21 (2009) 233201.
[10] T. Krenke, E. Duman, M. Acet, E.F. Wassermann, X. Moya, L. Manosa, A. Planes, Nat. Mater. 4 (2005) 450–454.
[11] Z.D. Han, D.H. Wang, C.L. Zhang, H.C. Xuan, B.X. Gu, Y.W. Du, Appl. Phys. Lett. 90 (2007) 042507.
[12] C. Jing, Z. Li, H.L. Zhang, J.P. Chen, Y.F. Qiao, S.X. Cao, J.C. Zhang, Eur. Phys. J. B 67 (2009) 193–196.
[13] T. Krenke, E. Duman, M. Acetc, X. Moya, L. Mañosa, A. Planes, J. Appl. Phys. 102 (2007) 033903.
[14] H.S. Liu, C.L. Zhang, Z.D. Han, H.C. Xuan, D.H. Wang, Y.W. Du, J. Alloys Compd. 467 (2009) 27–30.
[15] E.C. Passamani, F. Xavier, E. Favre-Nicolin, C. Larica, A.Y. Takeuchi, I.L. Castro, J.R. Proveti, J. Appl. Phys. 105 (2009) 033919.
[16] D.H. Wang, C.L. Zhang, H.C. Xuan, Z.D. Han, J.R. Zhang, S.L. Tang, B.X. Gu, Y.W. Du, J. Appl. Phys. 102 (2007) 013909.
[17] D.H. Wang, C.L. Zhang, Z.D. Han, H.C. Xuan, B.X. Gu, Y.W. Du, J. Appl. Phys. 103 (2008) 033901.
[18] C.L. Zhang, W.Q. Zou, H.C. Xuan, Z.D. Han, D.H. Wang, B.X. Gu, Y.W. Du, J. Phys. D: Appl. Phys. 40 (2007) 7287–7290.
[19] B. Gao, F.X. Hu, J. Shen, J. Wang, J.R. Sun, B.G. Shen, J. Magn. Magn. Mater. 321 (2009) 2571–2574.
[20] B. Gao, J. Shen, F.X. Hu, J. Wang, J.R. Sun, B.G. Shen, Appl. Phys. A 97 (2009) 443–447.
[21] Z. Han, R. Cui, X. Jiang, D. Wang, Y. Du, Chin. J. Rare Metals 34 (2010) 115–120.
[22] Y. Sutou, Y. Imano, N. Koeda, T. Omori, R. Kainuma, K. Ishida, K. Oikawa, Appl. Phys. Lett. 85 (2004) 4358–4360.